CrossMark

ORIGINAL ARTICLE

The effect of inhibition on stimulus-specific adaptation in the inferior colliculus

Yaneri A. Ayala[1,3] · Manuel S. Malmierca[1,2] (ID)

Abstract The inferior colliculus is a center of convergence for inhibitory and excitatory synaptic inputs that may be activated simultaneously by sound stimulation. Stimulus repetition may generate response habituation by changing the efficacy of neuron's synaptic inputs. Specialized IC neurons reduce their response to repetitive tones, but restore their firing when a different and infrequent tone occurs, a phenomenon known as stimulus specific adaptation. Here, using the microiontophoresis technique, we determined the role of $GABA_A$-, $GABA_B$-, and glycinergic receptors in stimulus-specific adaptation (SSA). We found that blockade of postsynaptic $GABA_B$ receptors selectively modulated response adaptation to repetitive sounds, whereas blockade of presynaptic $GABA_B$ receptors exerted a gain control effect on neuron excitability. Adaptation decreased when postsynaptic $GABA_B$ receptors were blocked, but increased if the blockade affected the presynaptic $GABA_B$ receptors. A dual, paradoxical effect was elicited by blockade of glycinergic receptors, i.e., both increase and decrease in adaptation. Moreover, simultaneous co-application of $GABA_A$, $GABA_{B,}$ and glycinergic antagonists demonstrated that local GABA- and glycine-mediated inhibition contributes to only about 50% of SSA.

Therefore, inhibition via chemical synapses dynamically modulate the strength and dynamics of stimulus-specific adaptation, but does not generate it.

Introduction

Response habituation (i.e., the reduction of a neural response after repetitive stimulation) is common in many brain regions, including the auditory system, accounting for non-linear encoding of stimulation probability (Carandini 2007; Maravall 2013; Winkler et al. 2009). A reduced response to a repetitive sound that is restored when a different sound is presented has been observed in the inferior colliculus (IC, Ayala and Malmierca 2013, 2014, 2015; Ayala et al. 2015; Duque et al. 2012, 2014; Malmierca et al. 2009), auditory thalamus (Anderson et al. 2009; Antunes et al. 2010; Calford 1983; Kraus et al. 1994), and auditory cortices (AC, Nieto-Diego and Malmierca 2016; Ulanovsky et al. 2003). This special type of adaptation is referred to as stimulus-specific adaptation (SSA). The SSA response to frequency deviants signals their probability of occurrence rather than their spectral content (Ulanovsky et al. 2003; Ayala and Malmierca 2013). The differential sensitivity to deviant and repetitive sounds is stronger in non-lemniscal regions of both subcortical (Antunes et al. 2010; Ayala et al. 2015; Duque et al. 2012; Malmierca et al. 2009) and cortical auditory areas (Nieto-Diego and Malmierca 2016).

The IC is the chief auditory midbrain center and is characterized by the convergence of excitatory, inhibitory, and neuromodulatory projections originating in the

✉ Manuel S. Malmierca
  msm@usal.es

[1] Auditory Neuroscience Laboratory, Institute of Neuroscience of Castilla Y León, University of Salamanca, C/Pintor Fernando Gallego, 1, 37007 Salamanca, Spain

[2] Department of Cell Biology and Pathology, Faculty of Medicine, University of Salamanca, Campus Miguel de Unamuno, 37007 Salamanca, Spain

[3] Present Address: Instituto de Neurobiología, Universidad Nacional Autónoma de México, Querétaro, Mexico

auditory brainstem and cortical regions as well as non-auditory centers (Ayala et al. 2015; Duque et al. 2014, 2015; Ito et al. 2015). These inputs are likely to contribute to the integration of information over time through changes in the efficiency of their synaptic connections based on their history of activation (Eytan et al. 2003; Friauf et al. 2015; Magnusson et al. 2008). For example, response habituation in the superior colliculus arises as a result of co-activation of excitatory and inhibitory neurons by the same retinal afferents (Binns and Salt 1995, 1997; Oyster and Takahashi 1975). In this case, the activation of GABAergic neurons prevents the response to subsequent presentations of the stimulus via $GABA_B$ receptors (Binns and Salt 1997). In the IC, it is well known that SSA is modulated by $GABA_A$-mediated inhibition (Pérez-González et al. 2012), acetylcholine (Ayala and Malmierca 2015) and endocanabinoids (Valdés-Baizabal et al. 2017). The blockade of $GABA_A$ receptors exerts an overall increase on neural excitability, affecting the response to both deviant and repetitive tones. Moreover, $GABA_A$-mediated inhibition decreases, but does not abolish SSA. Therefore, it is likely that additional synaptic inputs participate in the generation of response habituation evoked by the repetitive sounds.

Thus, the purpose of the present study was to determine the extent to which $GABA_B$ and glycinergic receptors and their combined activation with $GABA_A$ receptors contribute to SSA in IC neurons. To achieve this objective, we recorded single units and their responses to deviant and repetitive tones under the oddball paradigm. Responses were analyzed before and during the pharmacological manipulation of inhibitory receptors in anesthetized adult rats.

Materials and methods

Subjects and surgical procedures

Experiments were performed on 33 adult female rats (*Rattus norvegicus*; Long–Evans) with body weights ranging from 180 to 300 g. All surgical, recording, and histological procedures were conducted at the University of Salamanca, Spain. The experimental protocols were approved by Animal Care Committees of the University of Salamanca and followed the standards of the European Union (Directive 2010/63/EU) for the use of animals in neuroscience research. Detailed procedures were given previously (Hernandez et al. 2005; Malmierca et al. 2005, 2009). Urethane anesthesia was induced (1.5 g/kg, i.p., 20% solution) and given as needed (0.5 g/kg, i.p.) after hourly checking of the animal's eyeblink. Body temperature was monitored with a rectal probe and maintained at

38 ± 1 °C with a thermostatically controlled electric blanket. The trachea was cannulated, and atropine sulfate (0.05 mg/kg, s.c.; Braun) was administered to reduce bronchial secretions. Animals were connected to a ventilator (SAR-830/P; CWE Inc.), and expired CO_2 was monitored using a capnograph (Capstar-100; CWE Inc.). Finally, a midsagittal scalp incision was made, the muscle and underlying periosteum were scraped away, and a small hole was made on the left and right parietal bones to gain access to the IC. The dura was retracted and the exposed cortex was covered with 2% agar to prevent desiccation. Electrode penetrations were performed in both ICs with the aim to obtain the largest number of recorded neurons per animal. During the recording session, regular administration of saline or glucose solution (0.25 ml) was given subcutaneously to hydrate to the animals.

Acoustic delivery and electrophysiological recording

The animal was placed in a stereotaxic frame in which the ear bars were replaced by hollow specula that accommodated sound delivery system (Rees 1990) using two electrostatic loudspeakers (EC1, Tucker-Davis Technologies). Search stimuli were pure tones or white noise driven by a Tucker-Davis Technologies System 2 that was controlled by custom software for stimulus generation and on-line data visualization (Faure et al. 2003; Malmierca et al. 2008; Pérez-González et al. 2005, 2006). Action potentials were recorded with a Tucker-Davis Technologies BioAmp amplifier, the $10\times$ output of which was further amplified and bandpass filtered from 0.5 to 3 kHz (PC1, Tucker-Davis Technologies; frequency cut, 0.5–3 kHz) before passing through a spike discriminator (SD1, Tucker-Davis Technologies). Spike times were logged at 1 μs resolution on a computer by feeding the output of the spike discriminator into an event timer (ET1, Tucker-Davis Technologies) synchronized to a timing generator (TG6, Tucker-Davis Technologies). Extracellular single-unit responses were recorded in the left and/or right IC of each animal. The electrode was lowered into the brain with a piezoelectric microdrive (Burleigh 6000 ULN) mounted on a stereotaxic manipulator to a depth of 3.5–5 mm, where acoustically driven responses were found. The IC was approached from 20° relative to the frontal plane, so that the recording electrode moved caudally and ventrally during the penetration. After a neuron was isolated, pure tone stimuli with a duration of 75 ms (5 ms rise/fall time) were delivered to the contralateral ear to obtain the monaural frequency response area (FRA), i.e., the combination of frequencies and intensities capable of evoking a suprathreshold response. Five stimulus repetitions at each frequency (from 0.5 to 40 kHz, in 20–25 logarithmic steps)

and intensity (from 0 to 80 dB SPL, in 10 dB steps) were presented randomly at a repetition rate of 4 Hz.

Stimulus presentation paradigm

Pure tones (75 ms, 5 ms rise/fall time) were presented in an oddball paradigm similar to that used to record mismatch negativity responses in human studies (Näätänen 1992) and SSA in animal studies (Ulanovsky et al. 2003; Malmierca et al. 2009). Briefly, this paradigm consists of a flip-flop design using two pure tones at two different frequencies ($f1$ and $f2$), both of which elicit similar firing rates and response patterns at a level of 10–40 dB SPL above threshold within the neural FRA. For most neurons (64%), the $f1$ and $f2$ tones were located around the characteristic frequency (CF; the sound frequency that produces a response at the lowest stimulus level), whereas the rest of the frequency pairs were both either lower (23%) or higher (13%) than the CF. The frequency separations between $f1$ and $f2$ varied between 0.14 and 0.53 octaves. A train of 300 or 400 stimulus presentations containing both frequencies were delivered in two different sequences (sequences 1 and 2). The repetition rate of the train of stimuli was 4 Hz, as this was demonstrated previously to elicit SSA in IC neurons of the rat (Ayala and Malmierca 2013; Malmierca et al. 2009). In sequence 1, the $f1$ frequency was repetitively presented as the standard tone with a high probability of occurrence (90%) within the sequence. Interspersed randomly among the standard stimuli were the $f2$ frequency-deviant stimuli (10% probability). After the sequence 1 data set was obtained, the relative probabilities of the two stimuli were reversed, with $f2$ as the standard and $f1$ as the deviant in sequence 2.

Electrodes and microiontophoresis

A tungsten electrode (1–2.5 M; Merrill and Ainsworth 1972; Ayala et al. 2016) was used to record single-neuron activity. It was attached to a multibarrel borosilicate glass pipette that held drugs to be delivered in the vicinity of the recorded neuron. The tip of the recording electrode protruded 15–25 μm from the pipette tip. The glass pipette consisted of five barrels in an H configuration (World Precision Instruments, catalog no. 5B120F-4) with the tip broken to a diameter of 20–30 μm. The center barrel was filled with saline for current compensation (165 mM NaCl), whereas the others were filled with 20 mM strychnine hydrochloride (Sigma, catalog no. S-8753), 10 mM CGP 35348 hydrate (Sigma, catalog no. C5851), 10 mM of CGP 36216 hydrochloride (Tocris Bioscience, catalog no. 3219), or 20 mM gabazine (Sigma, catalog no. S106). Strychnine and gabazine are antagonists of the ionotropic glycine and $GABA_A$ receptors, respectively. The activation of both

receptors leads to influx of Cl^- ions that hyperpolarizes the postsynaptic cell and increases membrane conductance, thereby inhibiting neuronal activity (Hammond 2015). CGP 35348 and 36216 are antagonist of the metabotropic post- and pre-synaptic $GABA_B$ receptors, respectively. Activation of postsynaptic $GABA_B$ receptors results in the opening of K^+ conductances of the GIRK type and inhibition of Ca^{++} conductances producing a hyperpolarization. Activation of presynaptic $GABA_B$ receptors inhibits the release of a variety of different neurotransmitters, including glutamate and GABA mediated by a decrease in presynaptic Ca^{++} influx due to inhibition of presynaptic voltage-gated Ca^{++} channels (Mott 2015). The drugs were dissolved in distilled water and their pH adjusted to 3.5–4. All the compounds except CGP 36216 have been previously used in the mammalian IC (Kelly and Caspary 2005). The drugs were retained in the pipette with a – 15 nA current and were typically ejected, when required, using 30–40 nA currents (Neurophore BH-2 system, Harvard Apparatus). The duration of the drug ejection usually lasted 10–20 min, but could be extended when no visual effect was observed to ensure the absence of effect. After the drug ejection, we repeated the stimulation protocol until we observed recovery of neuronal firing.

Analysis of neural responses

For each neuron, the total raw number of spikes in response to the standard and deviant stimuli was normalized to the total number of deviant and standard trials to account for the different number of presentations in each oddball sequence. We used a default time window that included the entire stimulus duration (10–85 ms), but for cases where neurons exhibited a longer response latency and/or a sustained response, the window was adjusted by visual inspection of the peristimulus time histogram (PSTH) for each neuron to capture the extent of the spiking.

The degree of SSA was quantified by the Common-SSA Index (CSI) and the Frequency-Specific SSA Index (SI) reported previously (Antunes et al. 2010; Ayala and Malmierca 2013, 2014; Duque and Malmierca 2014; Duque et al. 2012; Malmierca et al. 2009; Pérez-González et al. 2012; Ulanovsky et al. 2003, 2004; von der Behrens et al. 2009). Both SSA indices reflect the difference between the neural responses to the deviant and standard stimuli, normalized to the sum of response to both stimuli, either averaging (CSI) or quantifying separately (SI) the responses to $f1$ and $f2$. The CSI is defined as

$$CSI = [d(f1) + d(f2) - s(f1) - s(f2)]/[d(f1) + d(f2) + s(f1) + s(f2)]$$

where $d(f)$ and $s(f)$ are responses to frequencies $f1$ or $f2$ when they were the deviant (d) or standard (s) stimulus, respectively. The SI was separately calculated for each frequency and it is defined as

$$\mathrm{SI}(fi) = [d(fi) - s(fi)]/[d(fi) + s(fi)], \quad i = 1, 2.$$

Positive CSI and SI values indicate that the neurons responded more strongly to the frequencies when they were deviant compared to when they were standard. Significant SSA level was indicated by indices larger than 0.1 (Ayala et al. 2013). To test for effects of the drugs on each individual neuron, the 95% bootstrap confidence intervals (CIs) for the baseline CSI were calculated using the *bootci* MATLAB function with 1000 bootstrap samples (Antunes and Malmierca 2011; Pérez-González et al. 2012). An effect of the drug was considered to be significant when the CSI value obtained under the ejection condition was larger or smaller than the high or low 95% CI, respectively.

The response latency and temporal pattern were also estimated for the responses to deviant and standard tones separately. The latency of the response was estimated as the average first spike latency (FSL) across deviant and standard trials. The response pattern was estimated by the population PSTH obtained from the average firing rate (spikes/second) across neurons for each drug group and each deviant and standard stimulus using a time bin size of 1 ms.

To characterize the temporal course of adaptation, we plotted the averaged response to the standard tone from all neurons as a function of the trial position. For each trial, the sum of the raw number of spikes was divided by the total number of deviant presentations that occurred at that trial (mean spikes per trial). The mean response was plotted at the original trial-long time scale. Then, we performed a nonlinear least-square fit to this population mean curve to find the best-fitting double exponential function as follows:

$$f(t) = A_{\mathrm{ss}} + A_{\mathrm{r}}.\mathrm{e}^{-t/\tau(\mathrm{r})} + A_{\mathrm{s}}.\mathrm{e}^{-t/\tau(\mathrm{s})},$$

where A_{ss}, A_{r} and A_{s} are the magnitudes of the steady state, and the rapid and slow components, respectively, τ_{r} and τ_{s} are the time constants of the rapid and slow components (Pérez-González et al. 2012; Pérez-González and Malmierca 2012).

Unless otherwise stated, data are presented as the median ± standard deviation. To test for significant differences among distributions of the strength and latency of the response to deviant and standard tone before and during drug application we performed the Friedman repeated measures analysis of variance on ranks. Post-hoc comparisons were performed following the Student–Newman

Keuls method. To test for drug effects on the SSA indices (SI, CSI), we performed the signed rank test, while to test for significant effects across groups of drug application, we performed the Kruskal–Wallis one-way ANOVA. Finally, to test for differences between the population PSTH before and during drug application, the Wilcoxon-signed rank test was performed between time bins of 5 ms. A p value < 0.05 was considered statistically significant. Analyses and figures were executed using SigmaPlot Version 11 (Systat Software, Inc., Chicago, IL, USA) and Matlab 13 (MathWorks, Inc., Natick, MA, USA).

Results

To test whether inhibitory inputs to SSA neurons in the IC mediate adaptation to repetitive sounds, we made single and combined microiontophoretic injections of GABAergic and glycinergic antagonists while recording extracellular single-unit activity. We recorded a total of 64 units, before, during, and after the application of CGP 36216 ($n = 15$), CGP 35348 ($n = 11$), strychnine ($n = 17$), CGP 35348 + gabazine ($n = 10$), and CGP 35348 + gabazine + strychnine ($n = 11$). Based on the firing pattern (Rees et al. 1990; Duque et al. 2012) and level of SSA (Malmierca et al. 2009; Ayala et al. 2013; Duque et al. 2012) exhibited by the recorded neurons, most of the neurons were located in the cortices of the IC (Malmierca et al. 2011). We found that (1) GABA$_B$-mediated inhibition modulates SSA in opposite directions depending on whether pre- or postsynaptic receptors are predominantly activated, (2) glycine-mediated inhibition has a paradoxical effect depending on the strength of SSA, and (3) concurrent GABAergic and glycinergic inhibition do not generate SSA in the IC. Descriptions of the effect of each drug administered separately are followed by descriptions of the effects of combinations of the drugs.

Effect of GABA$_B$ receptor blockade

In vitro studies demonstrated the presence of presynaptic GABA$_B$ receptors in the IC (Ma et al. 2002; Zhang and Wu 2000). To test the role of GABA$_B$ receptors in the generation of SSA in vivo, 20 oddball responses from 15 neurons were recorded under the local application of a specific antagonist for presynaptic receptors (CGP 36216). The neuron illustrated in Fig. 1a possesses a high level of SSA (CSI 0.92) with a typical onset-sustained response pattern showing a shorter response latency to the deviant (27.79 ms) than to the standard tone (36.44 ms; Duque et al. 2012). The application of CGP 36216 elicited a decrease in its excitability (Fig. 1a) and its CSI slightly increased to 0.94. After the injection, the discharge rate

increased above the baseline level, but the CSI (0.91) of this the neuron recovered to control values. The augmented firing discharge in the recovery condition can be due to the post-inhibitory rebound effect (Getting 1989). As shown by the single-neuron example as well as by the population response (Fig. 1b), CGP 36216 affected the strength of the onset and sustained components of the response to both deviant and repetitive tone. It decreased the spike count for the deviant tone from 1.3 ± 1.05 to 0.83 ± 0.96 spikes per stimulus (sps) and that for the standard tone from 0.56 ± 0.82 to 0.14 ± 0.79 sps (Fig. 1c, d, Friedman's test, $p < 0.05$). The population data for the recorded neurons exhibited different sensitivities for deviant and repetitive sounds with CSI and SI values ranging from -0.05 to 0.97 (Fig. 1e). At the population level, the drop in the evoked response resulted in a small, but significant increase of the SSA shifts the CSI from 0.45 to 0.48 and the SI from 0.45 to 0.46 (Fig. 1f, signed rank test, $p < 0.05$).

When we analyzed the FSL, the deviant responses were slightly increased (from 17.23 ± 8.54 to 17.89 ± 13.06 ms) by CGP 36216 application, while the FSL of the standard responses did not change and remained larger than deviant FSL (19.06 ± 11.48 ms, Friedman's test).

We also tested the effect of the commonly used GABA$_B$ receptor antagonist CGP 35348 which is known to have a much higher affinity for the post- than presynaptic receptors (Olpe et al. 1990). Figure 2a shows the effect of CGP 34358 on the responses of a single neuron which under control condition rapidly adapts its firing to the repetitive sound. The application of CGP 35348 increased the firing rate slowing the adaptation to the repetitive stimulus. As revealed by the bin comparison of average PSTHs, the responses to the deviant stimuli before and during the pharmacological manipulation remained virtually unchanged, while the sustained component of the response for the standard tone increased (Fig. 2b). Comparisons of spike counts from a total of 11 neurons revealed a weak but significant increase only in the responses to the repetitive (standard) stimuli, decreasing the difference between deviant- and repetitive-evoked responses from 26.56 in the baseline condition to 12.27% during CGP 35348 application (Fig. 2c, d, Friedman's test, $p < 0.05$). Likewise, the FSL of responses to the repetitive tone decreased from 30.85 ± 14.78 to 20.55 ± 14.44 ms, while the FSL of deviant responses remained the same (21.06 ± 13.22 ms) across conditions (Friedman's test). As shown in Fig. 2e, the great majority of SSA responses decreased regardless of the baseline SSA level (signed rank test, $p < 0.01$). Consequently, the CSI and SIs underwent a profound reduction dropping from 0.57 ± 0.38 to 0.29 ± 0.33 and 0.48 ± 0.37 to 0.11 ± 0.43 (Fig. 2f), respectively.

Effect of glycinergic receptor blockade

The response of 17 additional neurons to 23 pairs of frequencies during strychnine application was analyzed. Figure 3a, b shows the effect of strychnine on the response of an IC neuron that exhibited different degrees of SSA to two pairs of frequencies. The neuron had an onset pattern, whose strong level of SSA (CSI 0.95, panel a) was decreased by strychnine (0.82). This effect was due to an increase in the neuron's excitability. The spike count for deviant and standard tones slightly increased from 1.1 to 1.37 and from 0.01 to 0.08 sps, respectively. In contrast, partial SSA was elicited by the second pair of frequencies (CSI 0.46, panel b) during the baseline condition. Strychnine decreased the neuron's firing rate for the deviant (1.77–1 sps) and standard (0.38–0.1 sps) stimuli in different proportions, enhancing the saliency of the response to the deviant tone and increasing the CSI to 0.75. In both cases, the neuron maintained its onset firing pattern. This dual effect on the firing rate was also reflected at the population level (Fig. 3c) leading to an averaging out of the CSI (Fig. 3e, baseline 0.47 ± 0.37, strychnine 0.53 ± 0.34, signed rank test, $p = 0.73$), and SI (baseline 0.46 ± 0.37, strychnine 0.54 ± 0.34, $p = 0.59$). The CSI values ranged from -0.04 to 0.97 with the great majority being larger than 0.1 (17 out 23). In a more detailed analysis, we found that strychnine changed the SSA indices by 69% (red symbols, Fig. 3e, bootstrapping, CI 95%), but in contrast to the observed effect for the GABAergic antagonists (and as illustrated for the single neuron example), strychnine either increased (39%) or decreased (30%) similar percentages of SSA responses (Fig. 3e). Interestingly, we found that these different effects were CSI dependent, such that high baseline SSA indices (0.84 ± 0.28) were decreased (0.35 ± 0.27), whereas low baseline indices (0.46 ± 0.35) were increased (0.62 ± 0.35) by strychnine. Due to the opposite effects elicited by strychnine on SSA, the firing rates from both groups of responses were compared separately. We found that strychnine decreased the CSI of those neurons with high baseline SSA level by increasing the firing rate to both deviant (1.04 ± 0.42–1.44 ± 0.82 sps) and standard (0.17 ± 0.27–0.41 ± 0.32 sps) stimuli (Fig. 3d, f, signed rank test, $p < 0.05$). By contrast, strychnine increased the CSI of those neurons with low baseline CSI by decreasing the response to both deviant (1.83 ± 0.95–1.47 ± 1.36 sps) and standard tones (0.96 ± 0.84–0.75 ± 1.16 sps, Fig. 3d, f, signed rank test, $p < 0.05$). The FSL for both groups remained unchanged by strychnine and did not differ between them (deviant 16.52 ± 7.26 ms, standard 17.62 ± 13.22 ms).
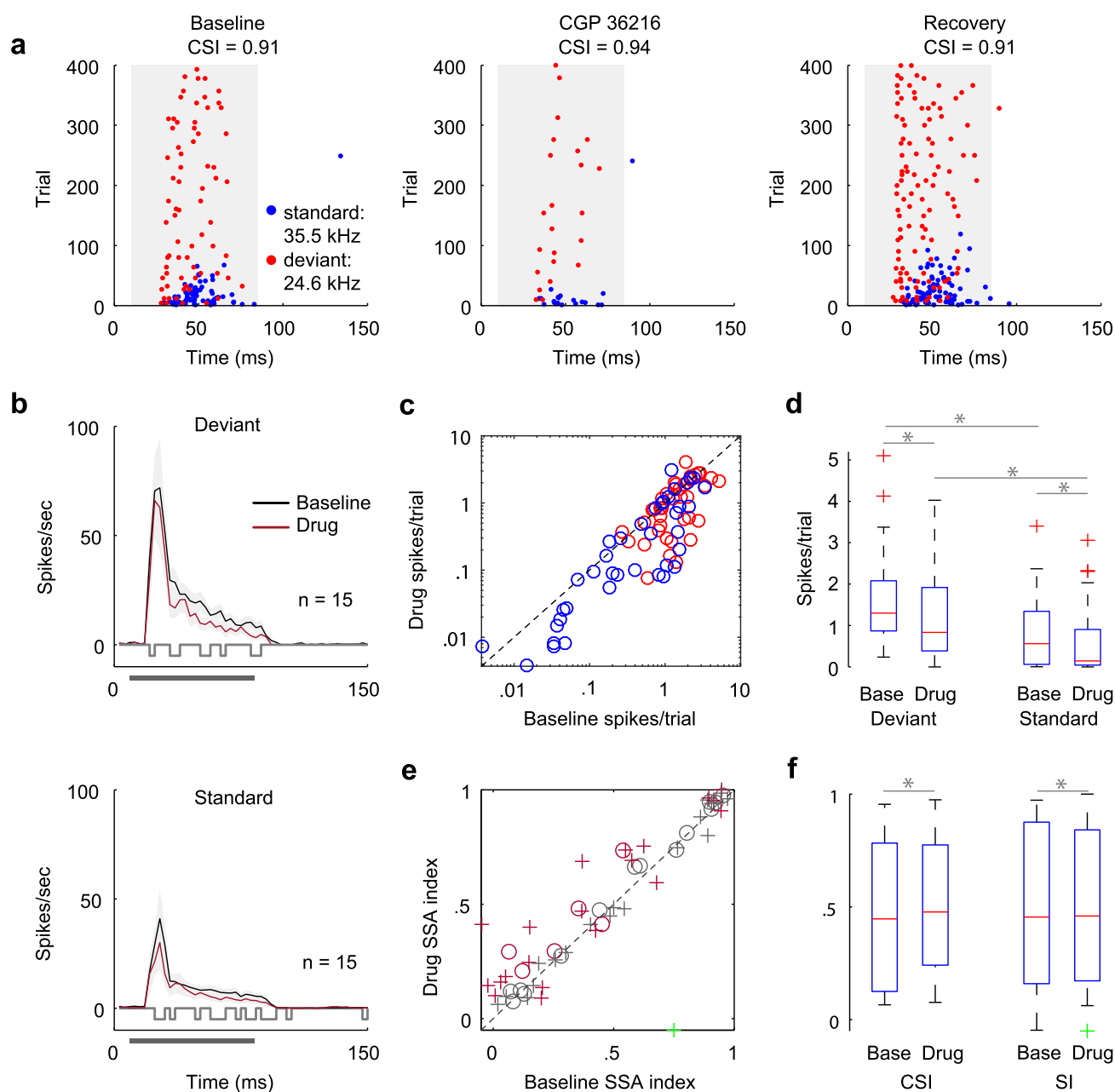
Fig. 1 CGP 36216 effect on neural sensitivity. **a** Dot raster of the response to deviant (red) and standard (blue) sound frequencies before (baseline), during (CGP 36216), and after (recovery) the microiontophoretic application of CGP 36216. The CSI for that pair of frequencies is showed in the top of each raster. Deviant trials corresponded to the 10% of trials randomly interspersed with standard trials. **b** Population peristimulus-time histograms of the response to deviant and standard stimuli before and during the drug application. Significant difference between bins (bin size = 5 ms) is indicated by the negative y values at the bottom line plot (Wilcoxon-signed rank test, $p < 0.05$). Tone duration (75 ms) is indicated by the filled bar. The number neurons included in each histogram is indicated, but note that responses to at least two tones were measured for each neuron. **c** Comparison of the mean spike count (spikes/trial) for deviant and

standard stimuli before and during the CGP 36216 injection. **d** Box plots showing the distribution of the spike count in both conditions, baseline (base), and drug application. The red lines within each box represent the median values, the edges of the box delimit the 25th and 75th percentiles, the whisker bars extent to the 10th and 90th percentiles, and the crosses represent outlier values. Differences tested with the Friedman's test. $*p < 0.05$. **e** Comparison of the CSI (circles) and SI values (crosses) before and during drug application. Gray symbols represent those values not significantly different between conditions (Bootstrapping, 95% CI). **f** Box plot of the SSA values, same format as **d**. Differences between SSA indices were tested with the signed rank test ($p < 0.01$). Green symbols in panels **e** and **f** represent values falling out of the x-axis interval
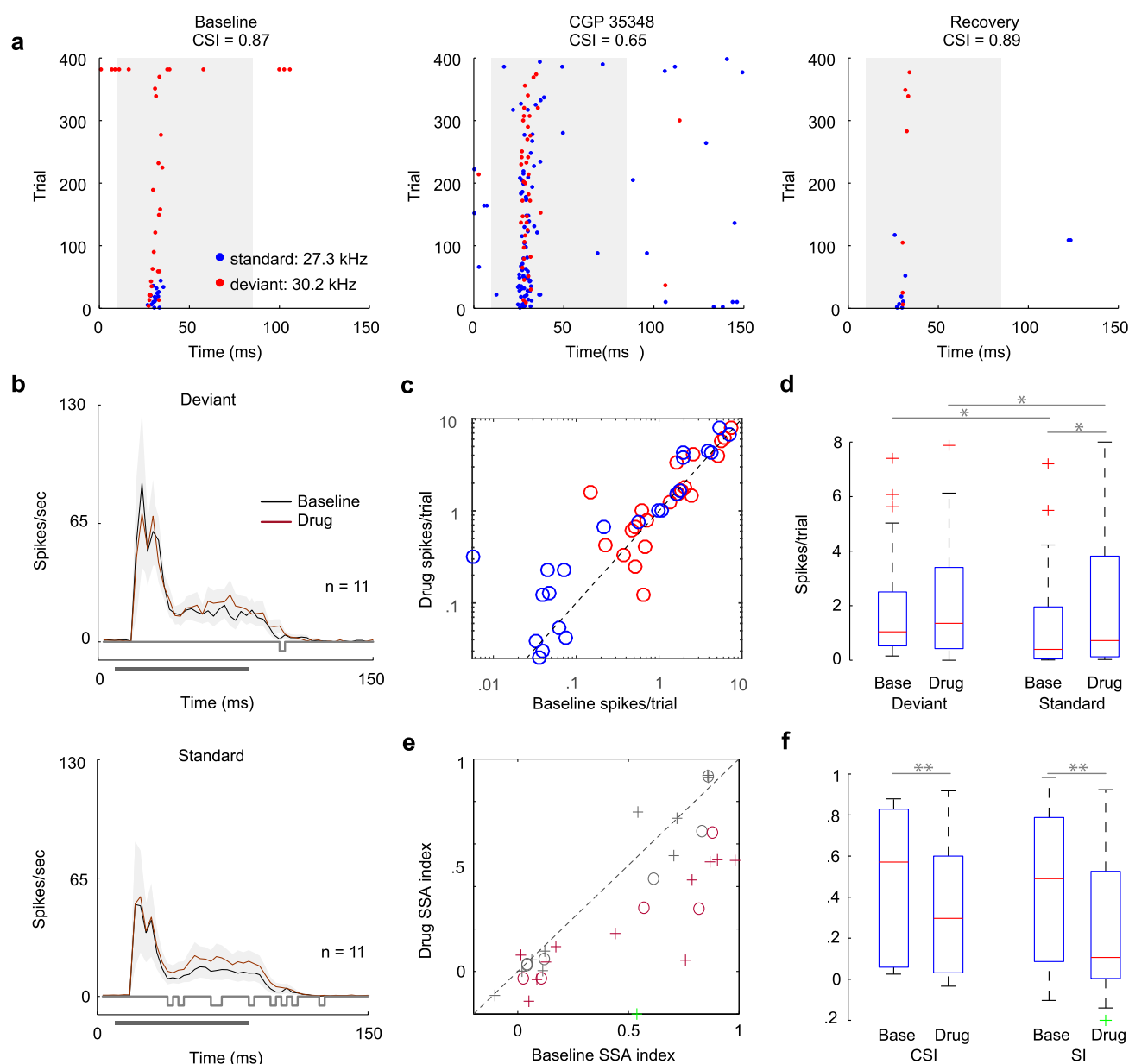
Fig. 2 CGP 35348 effect on neural sensitivity. **a** Single neuron response to deviant and standard tone before, during, and after the blockade of post-synaptic GABA$_B$ receptors. **b** Population peristimulus-time histograms of the response to deviant and standard stimuli before and during the drug application. **c, d** Single-neuron and population spike count before and during drug application. **d, e** Single-neuron and population SSA indices before and during drug application. Same format as in Fig. 1. *$p < 0.05$, **$p < 0.01$

Combined injections

The most plausible scenario is that multiple inhibitory inputs are simultaneously activated under repetitive stimulation, affecting different receptor types. Thus, to explore whether specific adaptation to repetitive sounds was due to a synergistic activation of several inhibitory inputs, we co-applied different inhibitory antagonists to the same IC neuron. First, we made combined injections of CGP 35348 and gabazine, since both drugs decreased the CSI as revealed by the results described above (Fig. 2) and

previous studies (Pérez-González et al. 2012). Figure 4a illustrates the effect of the joint application for CGP 35348 and gabazine on a single-neuron's response to the oddball stimulation. This neuron became more responsive under the blockade condition firing more to standard trials (from 28 to 133 out a total of 360) and increasing its response strength as well (from 0.1 to 0.48 sps). The effect was almost completely reversed during the recovery period (right panel of Fig. 4a). A total of ten neurons were recorded in this condition. Analogous to the single-neuron observation, there were robust increases in the magnitude
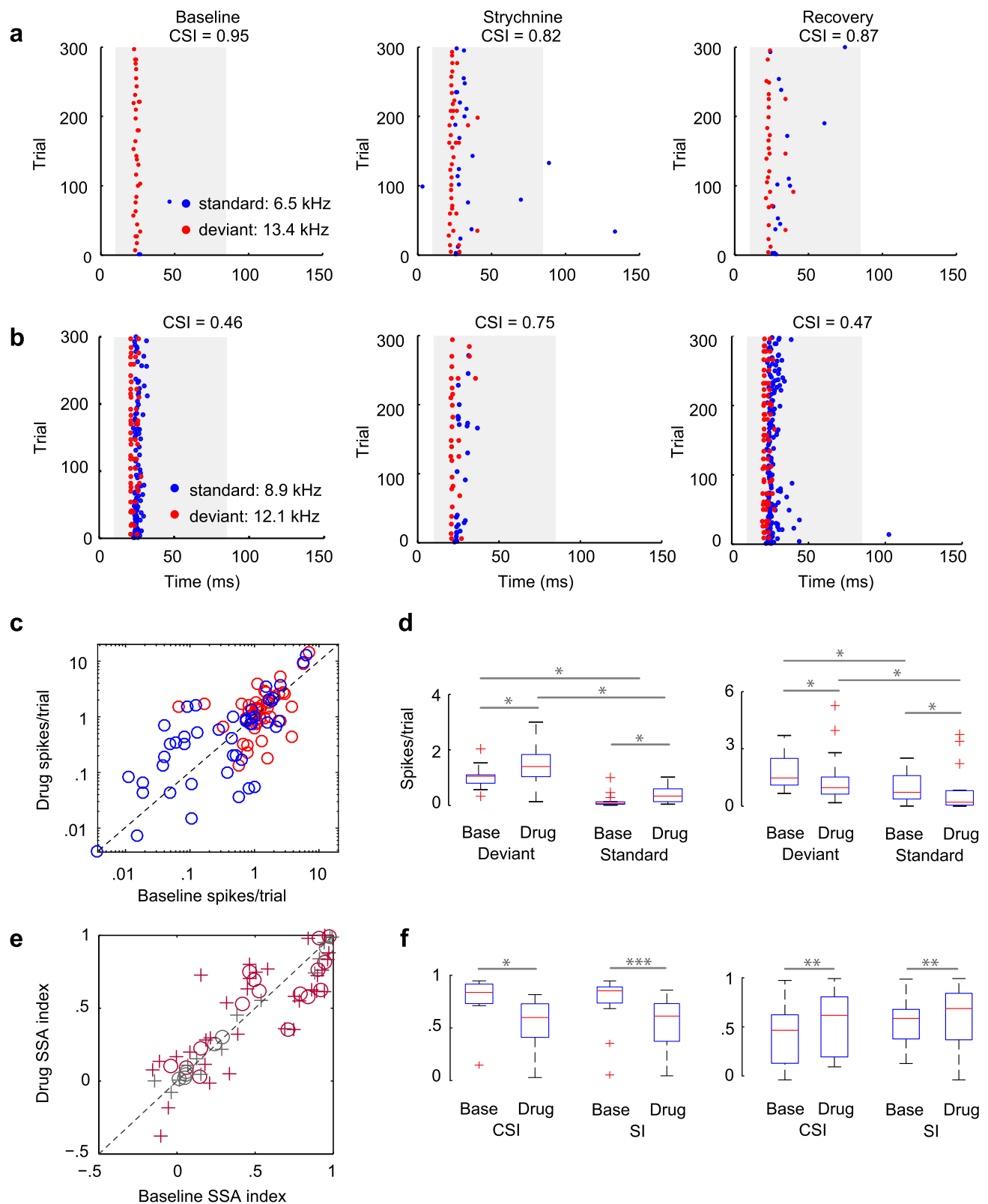
Fig. 3 Strychnine effect on neural sensitivity. **a**, **b** Dot raster of the response to two pairs of frequencies when delivered frequent or infrequently from the same IC neuron. **c** Single neuron and population spike count before and during antagonist application. **d** Boxplots of the population response for those neurons that increased (left) or decreased (right) their firing response. **e** Single neuron and population SSA indices before and during application of antagonist. **f** Population SSA indices for neurons whose SSA strength decreased (left) or increased (right). Same format as in Fig. 1. *$p < 0.05$, **$p < 0.01$
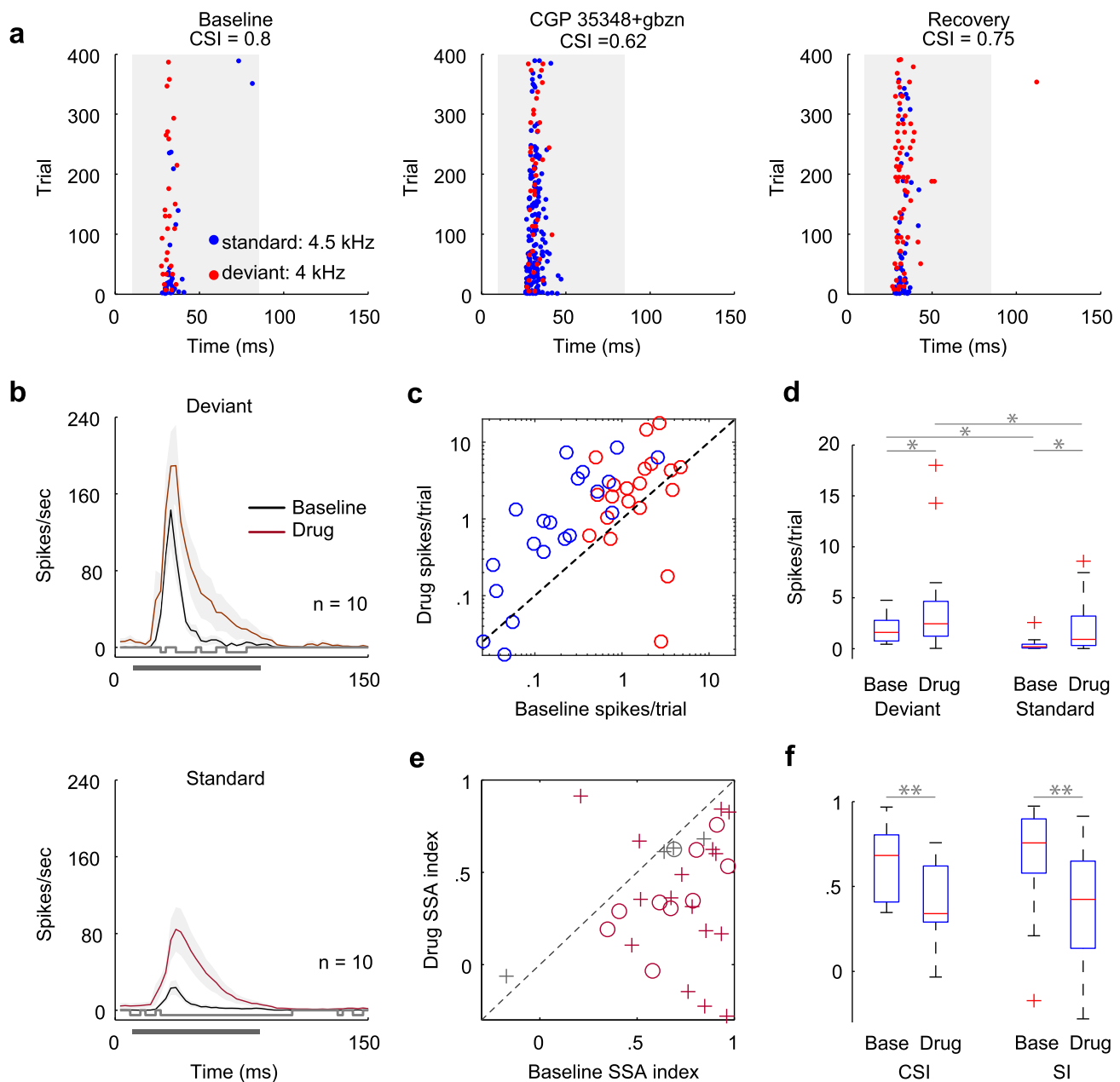
Fig. 4 Effect of the combined application of CGP 35348 and gabazine (gbzn) on neural sensitivity. **a** Dot rasters from a single unit neuron showing the response to deviant and standard tones before, during, and after the blockade of postsynaptic GABA_A and GABA_B receptors. **b** Population peristimulus-time histograms of the response to deviant and standard stimuli before and during the drug application. **c** Single-neuron and **d** population spike count of the response to deviant and standard tones before and during drug application. **e, f** Single neuron and population SSA indices before and during drug application. Same format as in Fig. 1. $*p < 0.05$, $**p < 0.01$

and duration of the responses to deviant and repetitive tones resulting in significant differences between the population PSTHs (Fig. 4b). Augmented response duration is a typical effect of gabazine on SSA neurons (Pérez-González et al. 2012). In addition, the FSLs for both tones were reduced (deviant 20.62 ± 7.24 vs. 19.77 ± 8.21 ms, standard 23.24 ± 10.09–21.61 ± 6.45 ms), but the difference

between deviant and standard tone was not abolished (Friedman's test). The great majority of responses to deviant and repetitive sound (33 out 40; Fig. 4c) augmented, and consequently, the population spike count also increased (Fig. 4d). The response strength increased from 1.6 ± 1.26 to 2.45 ± 4.58 sps and from 0.18 ± 0.58 to 0.91 ± 2.63 sps for deviant and standard stimulus,
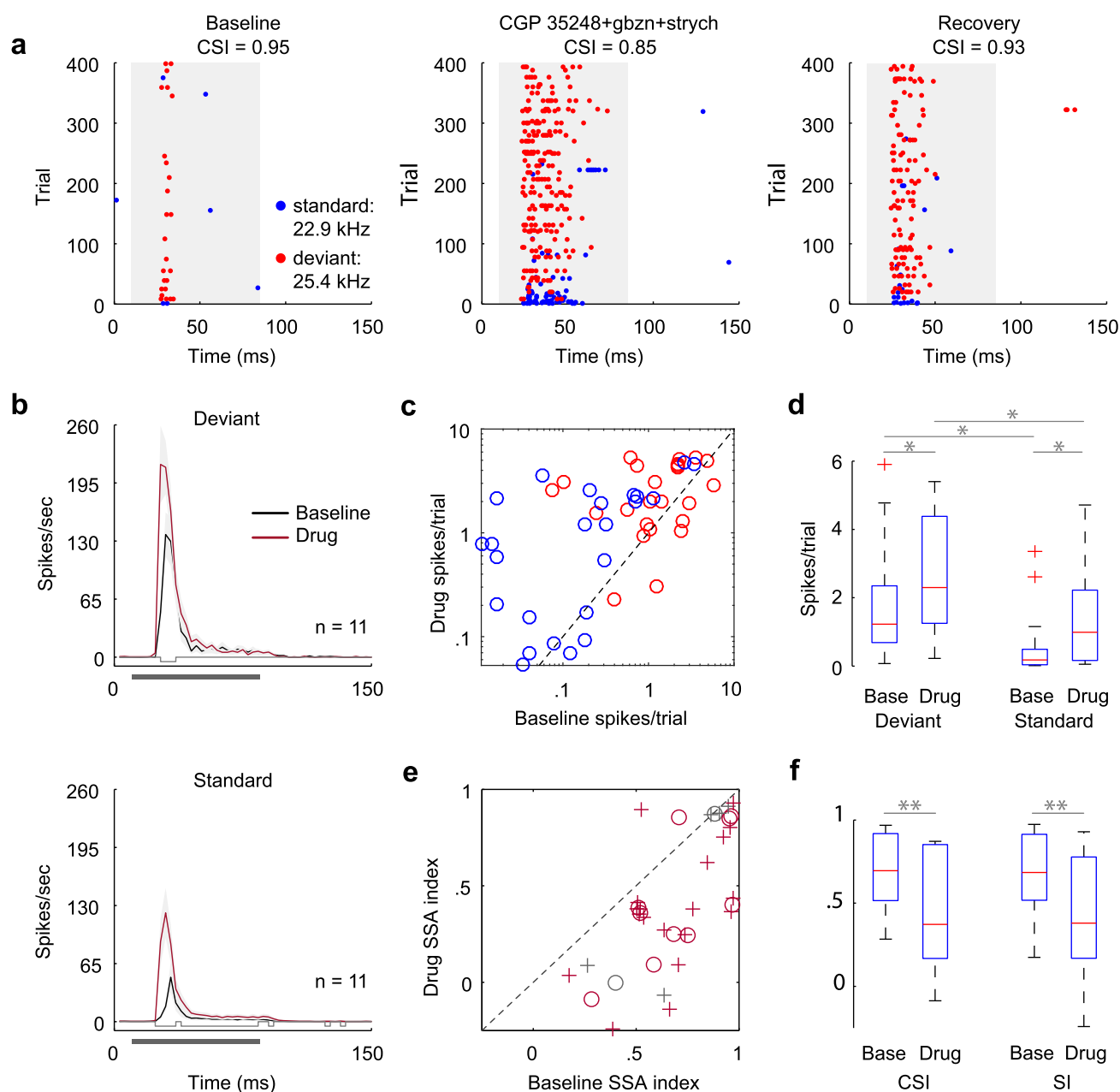
Fig. 5 Effect of the combined application of CGP 35348, gabazine (gbzn), and strychnine (strych) on neural sensitivity. **a** Dot rasters from a single unit neuron showing the response to deviant and standard tones before, during and after the blockade of postsynaptic GABA$_A$ and GABA$_B$ receptors. The blockade of GABAergic and glycinergic receptors changed the magnitude and temporal pattern of the response. **b** Population peristimulus-time histograms of the response to deviant and standard stimuli before and during the drug application. **c** Single neuron and **d** population spike count of the response to deviant and standard tones before and during drug application. **e** Single neuron and **f** population SSA indices before and during drug application. Same format as in Fig. 1. *$p < 0.05$, **$p < 0.01$

respectively (Friedman's test, $p < 0.05$). As predicted from the low firing to standard sounds, these neurons exhibited high levels of SSA. The population of CSI values ranged from 0.35 to 0.97 (Fig. 4e). Both CSI and SI were profoundly affected by the GABAergic antagonists and decreased by 51.23 and 43.93%, respectively (Fig. 4f, signed rank test, $p < 0.01$).

Finally, to rule out that the join activation of both GABAergic and glycinergic receptors generates the adaptation to the repetitive tone, we co-applied the antagonists for the three inhibitory receptors, i.e., GABA$_B$ (CGP 35348), GABA$_A$ (gabazine), and glycinergic receptors (strychnine). We excluded CGP 36216, since it augmented the SSA. Combined GABAergic and glycinergic blockade

exerted even a much greater change in the neuron's excitability than the application of any of these drugs alone. As illustrated in Fig. 5a, the response pattern of the example neuron changed from an onset discharge with an FSL of 19.85 ms to a longer duration, sustained response with a shorter FSL (16.22 ms). Despite the obvious change in the neuron's responsiveness, its high SSA level (CSI 0.95) was not abolished by the multiple inhibitory blockade, only decreased to 0.85 which recovered to 0.93 after blockade as displayed in the right panel. The augmented excitability was also evident in the average population response pattern (Fig. 5b) and spike count (Fig. 5c, d) from 12 oddball responses of 11 IC neurons. The onset component of the response for deviant tones was mainly affected, while both the phasic and sustained components of the responses to the standard tone were increased, as revealed by a bin-to-bin comparison (Fig. 5b, signed rank test, $p < 0.05$). The spike count increased from 1.22 ± 1.46 to 2.3 ± 1.68 sps for the deviant stimulus and from 0.18 ± 0.83 to 0.99 ± 1.42 sps for the standard one. The combined blockade also shortened the FSLs for deviant (18.68 ± 2.07 vs. 16.87 ± 2.22 ms) and repetitive stimulus (20.39 ± 5.85 vs. 17.95 ± 4.07 ms). Despite the evident change in the neural excitability, the deviant tone continued to elicit a stronger response with smaller FSLs during the blockade condition. The CSI and SI values decreased by 83 and 79%, respectively, and were significantly affected by the injections, clustering below the diagonal line (Fig. 5e). The CSI population values decreased from 0.69 ± 0.23 to 0.37 ± 0.35, while the SI decreased from 0.68 ± 0.23 to 0.38 ± 0.35 for the SI (signed rank test, $p < 0.01$).

Comparison across blockade groups

Figure 6a shows the normalized change in the spike count across the five blockade conditions. Combined injections of GABAergic and glycinergic antagonists elicited a greater change in firing rate than the injection of CGP35348 or strychnine alone. Significant differences only emerged across responses to the standard sound, indicating that a larger amount of inhibition is recruited by standard tones (Kruskal–Wallis test, $p < 0.05$). The greatest decrease in CSI was exerted by CGP 35348 (58%) due to its differential increase on the response to the standard sound without affecting the response to the deviant sound as also occurred in combined injections, although it did not reach a significant difference (Kruskal–Wallis test, $p > 0.05$, Fig. 6b). By contrast, and also surprisingly, CGP 36216 decreased the neuronal responsiveness for deviant and standard tones by 22 and 32%, respectively, and increased the CSI by 29%.
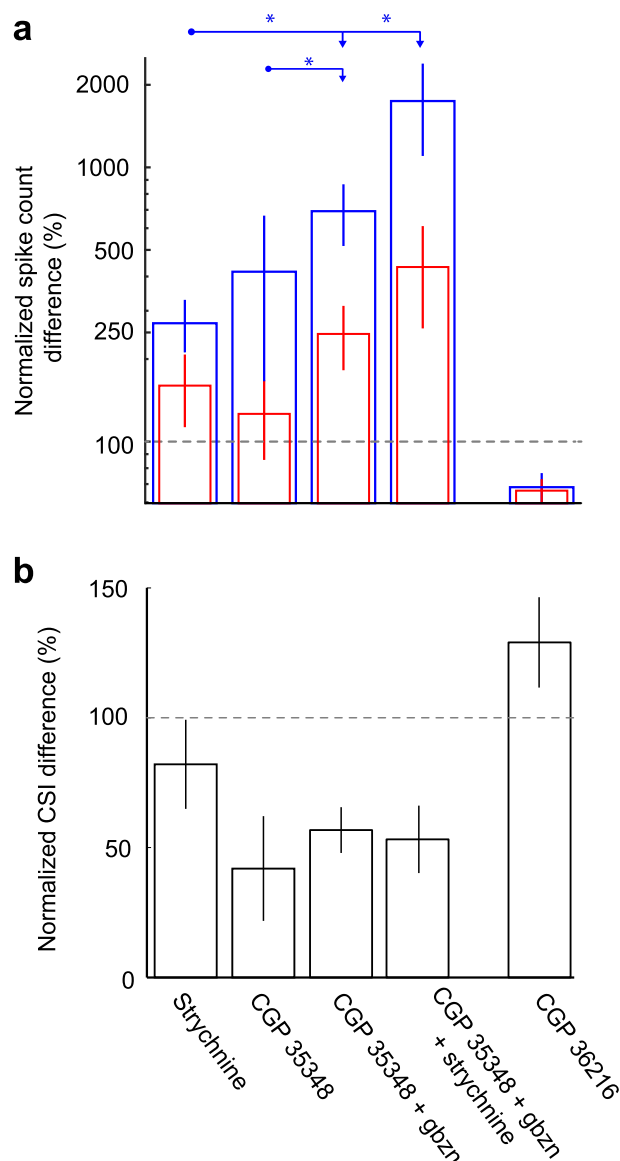
Fig. 6 Comparison of the drug's effect on neuronal response and SSA level. **a** Normalized spike count difference expressed in percentage among drug groups for deviant (red) and standard (blue) frequencies. The mean value is represented by the bar height and the whiskers indicate the standard error. Dashed line indicates the baseline value (100%). **b** Bar plot of the normalized CSI differences. Same format as **a**. Kruskal–Wallis test used for group comparisons. *$p < 0.05$

Effect on the time course

The time course of adaptation for all drugs and for combined injections which exerted a unidirectional effect on the population of neurons was fitted to a double exponential function (Pérez-González et al. 2012), which includes a fast and slow decay as well as a steady-state component. The magnitude and time constants for the three components are reported in Table 1. The combined

Table 1 Time course of adaptation

	A_r	A_s	A_{ss}	τ_r	τ_s	r^2
Baseline	2.56 (1.18, 3.94)	0.44 (0.34, 0.55)	0.75 (0.74, 0.77)	1.04 (0.52, 1.55)	27.77 (19.14, 36.39)	0.62
CGP 36216	2.5 (.15, 4.84)	0.35 (0.27, 0.43)	0.54* (.53, 0.55)	0.76 (0.24, 1.28)	28.5 (19.47, 13.52)	0.56
Baseline	5.69 (2.68, 8.70)	0.79 (0.53, 1.06)	1.38 (1.35, 1.41)	1.04 (0.51, 1.56)	23.88 (13.79, 33.97)	0.57
CGP 35348	3.1 (0.76, 5.43)	0.99 (0.37, 1.61)	1.76* (1.73, 1.79)	1.26 (0.02, 2.51)	12.95 (5.09, 20.81)	0.45
Baseline	5.97 (4.36, 7.57)	1.15 (1.02, 1.26)	0.30 (0.28, 0.32)	1.02 (0.77, 1.28)	28.35 (24.42, 32.29)	0.88
CGP 35348 + gabazine	6.28 (3.65, 8.90)	2.18* (1.70, 2.66)	1.96* (1.91, 2.01)	1.54 (0.72, 2.36)	26.46 (19.61, 33.31)	0.70
Baseline	8.45 (5.51, 11.38)	0.82 (0.72, 0.92)	0.39 (0.37, 0.40)	0.79 (0.59, 1)	36.38 (29.92, 42.84)	0.84
CGP 35348 + gabazine + strychnine	5.17 (3.52, 6.82)	1.11* (1.01, 1.21)	1.18* (1.11, 124)	1.38 (0.93, 1.83)	81.63* (62.07, 101.2)	0.78

The temporal course of the response to the standard stimuli was fitted to a double exponential function containing the following parameters: magnitude of the fast decay component (A_r), magnitude of the slow decay component (A_s), magnitude of the sustained component (A_{ss}), tau of the fast decay component (τ_s), and tau of the slow decay component (τ_s). Median value and the 25th–75th percentile are reported for each parameter. The goodness of the fit is indicated by r^2. Significant differences of the parameter values between baseline and drug condition are indicated by asterisks

injection of antagonists of GABA$_A$, GABA$_B$, and glycinergic receptors increased the slow and sustained components of adaptation by 35 and 202%, respectively. Single antagonist applications only affected the sustained component. Application of CGP 35348 increased the sustained component by 27%, whereas CGP 36216 decreased it by 28%.

Discussion

We assessed whether the removal of local GABAergic and/or glycinergic inhibition abolishes SSA in IC neurons. The contribution of inhibitory receptors was tested using single or combined injections of the GABA$_B$ (CGP 35348 and CGP 36216), GABA$_A$ (gabazine), and glycinergic receptors (strychnine) antagonists in the vicinity of the recorded neurons. Our results indicate that SSA is not generated by GABAergic and/or glycinergic inhibitions, but that SSA is increased or decreased according to the receptor type that is manipulated. In the following, we discuss these main findings and their functional significance.
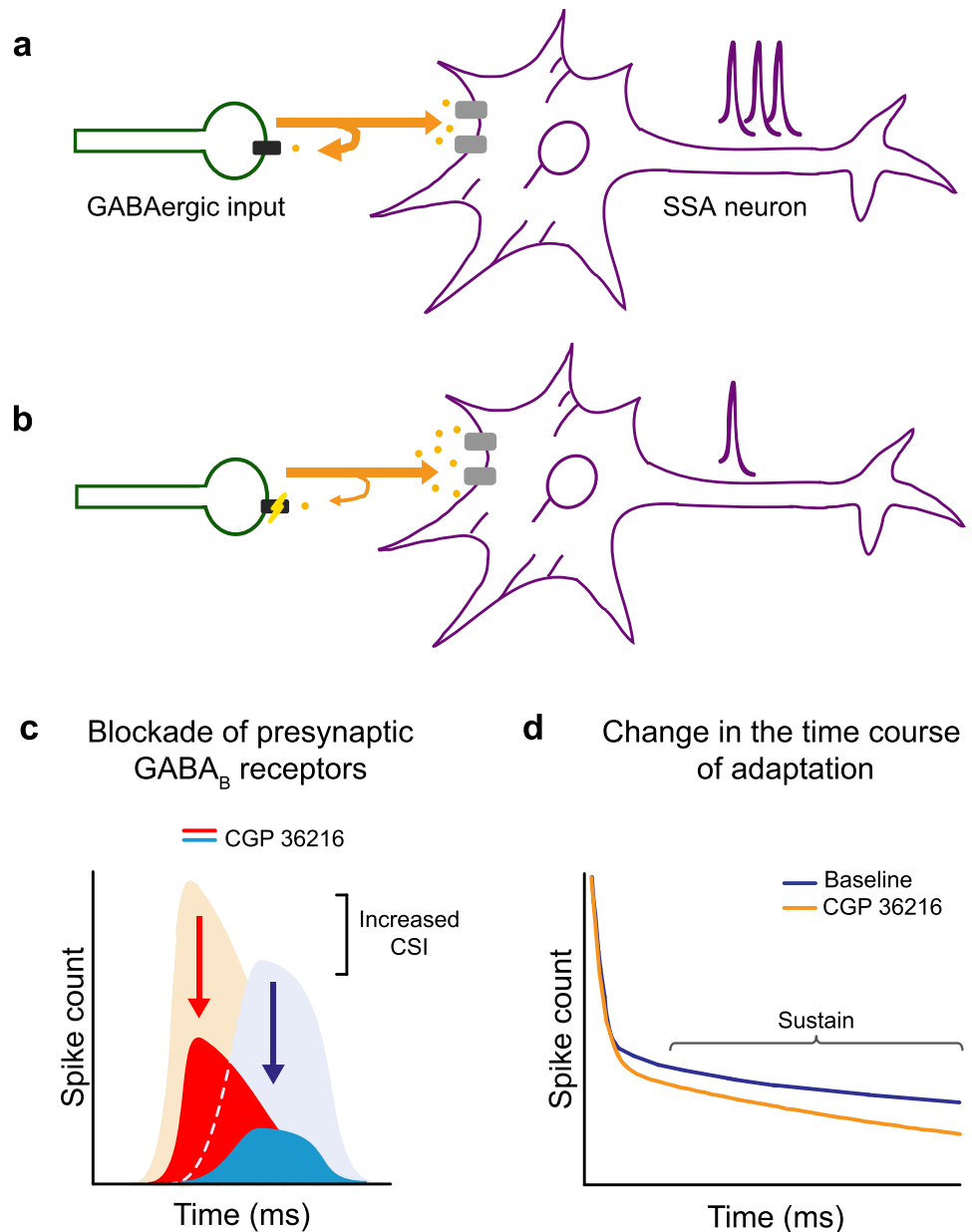
Histological (Jamal et al. 2011, 2012; Milbrandt et al. 1994) and in vitro physiological studies (Ma et al. 2002; Sun et al. 2006; Sun and Wu 2008, 2009) indicate that GABA$_B$ receptors are expressed both pre- and post-synaptically in the IC of the rat. We found opposite effects on neural responsiveness in the IC elicited by two GABA$_B$ antagonists, namely, CGP 36216 and CGP 35348, but none of them was involved in the generation of SSA. CGP 36216 is a relatively new and selective antagonist for presynaptic GABA$_B$ receptors (Ong et al. 2001), while the CGP 35348 has been widely used to block both postsynaptic and presynaptic receptors in auditory centers (Luo et al. 2011; Magnusson et al. 2008; Sun et al. 2006) although with a

much higher affinity for postsynaptic receptors (Staubli et al. 1999). To the best of our knowledge, this is the first in vivo study using CGP 36216 to manipulate neuronal excitability.

The blockade of pre-synaptic GABA$_B$ receptors by CGP 36216 exerted a gain control on SSA by decreasing the neuron's overall excitability (Figs. 1, 6). Previously, GABA$_B$ receptors have been demonstrated to act as autoreceptors at GABAergic terminals in the rat IC, whose activation suppresses GABAergic inhibition (Ma et al. 2002; Zhang and Wu 2000). For example, Ma et al. (2002) observed that a GABA$_B$ agonist, baclofen, decreases the amplitude of the inhibitory postsynaptic currents without increasing the neuron's membrane conductance demonstrating that bacoflen effect is exerted on activation of presynaptic receptors. Therefore, the suppressive effect elicited by CGP 36216 might result from the blockade of presynaptic GABA$_B$ receptors located at GABAergic terminals which would exert an overall inhibition on SSA neurons (Fig. 7a). Thus, CGP 36216 would allow a continuous GABA release on SSA neurons, decreasing their firing rate (Fig. 7b) and maximizing the contrast between deviant and standard responses and, therefore, increasing the CSI (Fig. 7c). A plausible role of this GABAergic inhibition on SSA neurons would be to shape their characteristic sound response pattern, i.e., onset and low firing response (Duque et al. 2012).

By contrast, CGP 35348 exerted a subtle modulation of SSA by increasing the response to the standard tone alone without affecting the response to the deviant tone and, therefore, decreasing the CSI (Figs. 2, 6). Previous in vivo (Burger and Pollak 1998; Faingold et al. 1991; Vaughn et al. 1996) and in vitro studies (Sun and Wu 2009) using CGP 35348 have reported that CGP 35348 elicits an increase in neuronal excitability by decreasing the

Fig. 7 Schematic representation of hypothetical inputs to SSA neurons and distribution of GABA$_B$ receptors underlying the CGP 36216 effects. **a** Activation of presynaptic GABA terminals would activate the GABA$_B$ autoreceptors (black rectangles) increasing the neuronal excitability of SSA neurons. **b** CGP 36216 blocks the auto-inhibition of GABAergic terminals, thereby increasing the release of GABA and decreasing excitability of SSA neurons by activating more postsynaptic GABAergic receptors (gray rectangles). **c, d** Augmented inhibition decreases the overall neuronal excitability decreasing the response to deviant (red) and standard tone (blue) and accentuating the sustained component of adaptation
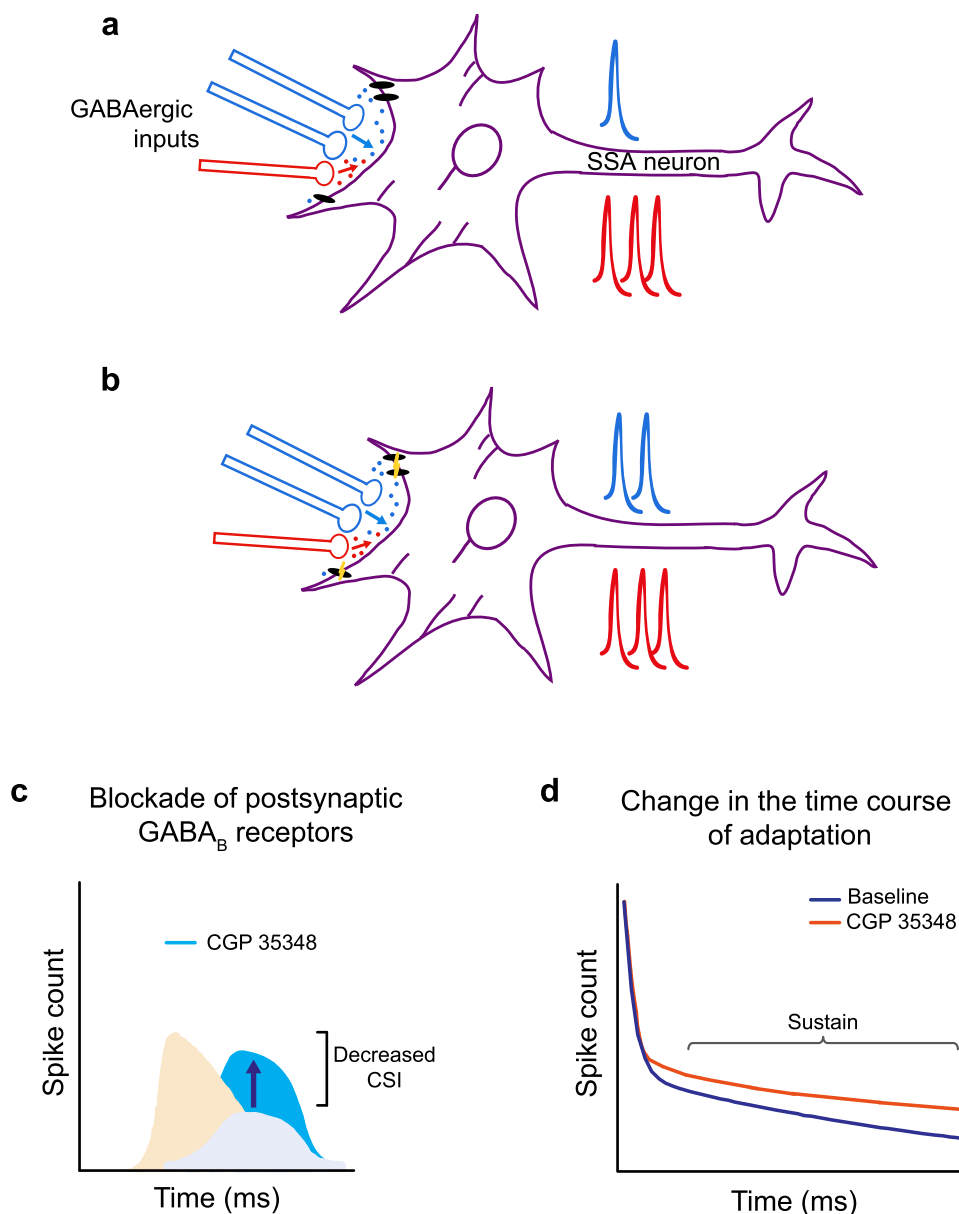

membrane threshold for the generation of action potentials. The selective effect on the response to standard tone could be explained by assuming that (1) GABA$_B$ postsynaptic receptors on SSA neurons have a mainly extrasynaptic location and that (2) standard tone recruit larger amount of GABA release than deviant tone by activating more inhibitory inputs (Fig. 8a). Therefore, only when sufficient amount of GABA is released by the standard tone stimulus, the inhibitory neurotransmitter spillovers the synaptic cleft reaching the extrasynaptic GABA$_B$ receptors (Fig. 8b). Consequently, the binding of CGP 35348 antagonist on those receptors only diminishes the response evoked by the standard tone (Fig. 8c). Extrasynaptic GABA$_B$ receptors have been described in brain regions including the globus

pallidus (Charara et al. 2005) and hippocampus (Pham et al. 1998; Scanziani 2000). Likewise, the activation of different sets of afferents by deviant and standard sound frequencies has been previously hypothesized (Nelken 2014) and modeled (Duque et al. 2016). The ascending channels activated by the frequent and infrequent tones could also recruit different sets of inhibitory inputs. Future in vitro studies (e.g., Wang et al. 2014) dissecting SSA neuronal circuitry (Ayala et al. 2015) will be necessary to probe the receptor location and mechanisms of action of these antagonists.

While GABA$_B$ receptor antagonists exerted a unidirectional effect on CSI (same direction of effect on 75–100% measures), strychnine elicited a heterogeneous effect on

Fig. 8 Schematic representation of hypothetical inputs to SSA neurons and distribution of GABA$_B$ receptors underlying the CGP 35348 effects. **a** In this model, responses to standard and deviant tone would recruit different sets of GABAergic inputs and different amounts of inhibition. Postsynaptic GABA$_B$ receptors (black cylinders) would be mostly located at extrasynaptic sites on SSA neurons. Standard tones would constantly activate the GABAergic inputs (blue inputs) leading to a spillover of GABA neurotransmitter that in turn would activate the extrasynaptic GABA$_B$ receptors. By contrast, GABA release triggered by rarely occurring deviant tones (red inputs) would be insufficient to reach the extrasynaptic receptors. **b, c** Blockade of the GABA$_B$ receptors by CGP 35348 would only decrease the inhibition elicited by repetitively activated GABAergic inputs (blue), thereby increasing the neuronal response to standard sounds while not affecting the response to deviant ones (red). **d** Slow dynamics of the metabotropic GABA$_B$ receptors as well as the dynamics of GABA to reach the extrasynaptic receptors would contribute to the late effect of CGP 35348 on the sustained component of adaptation

SSA (Fig. 3), increasing or decreasing CSI by 56 or 44%, respectively. Strychnine modified both the firing rate and SSA in a baseline-dependent manner similar to the effect of cholinergic receptors (Ayala and Malmierca 2014), suggesting that SSA strength is shaped by differential sets of inputs and/or differential combinations of neuronal receptors. The strychnine effect on SSA contrasts with its typical excitatory effect on tone-evoked responses previously described (Dimitrov et al. 2014; LeBeau et al. 2001). The removal of glycine-mediated inhibition affects the neuron's sensitivity to both deviant and standard tones, but increases response to tones that elicit strong SSA in the control condition, while decreases response to those that elicit partial SSA. To the best of our knowledge, this is the first examination of the effect of glycine receptors on SSA and

the first report of a paradoxical effect of strychnine in the IC. We can argue that this paradoxical effect is not due to a nonspecific effect of pH or current injections, since strychnine did not affect 6 out of 17 recorded neurons. Moreover, strychnine increases or decreases the responses to different sets of frequencies in the same neuron, as the one illustrated in Fig. 3. A differential effect of glycine in different parts of the receptive field of IC neurons has been suggested to occur in bats (Williams and Fuzessery 2011). Responses to low-frequency tones appear to be shaped by both GABAergic and glycinergic inputs, whereas the high-frequency region is affected exclusively by glycinergic input. Whether a frequency-dependent distribution of glycine inhibition or a differential co-expression with other types of inputs accounts for the paradoxical effects

observed remain to be determined in future studies. We failed to find any correlation between neuronal response features and the direction of the effect due to insufficient data. A second explanation for the observed paradoxical effects is a spread of strychnine beyond glycinergic receptors on the SSA neuron, affecting its sources of inputs as well.

The third main finding of our study is that when multiple inhibitory receptors were blocked, augmented effects were evident (Figs. 4c, d, 5c, d). It is well known that GABA$_A$ receptors regulate the postsynaptic membrane potential (Sivaramakrishnan et al. 2004), while GABA$_B$ receptors can increase or decrease the excitability of neurons by acting on pre- and post-synaptic receptors as shown above. Comparisons of the normalized changes elicited by co-application of antagonists on population responses demonstrate that the gradual increase of neuronal responsiveness was only significant on the response to the repetitive stimulus. This result indicates that the recruitment of inhibitory inputs has a major impact on neural adaptation elicited by stimulus repetition rather than in the modulation of sound-evoked responses (Fig. 6a). Results also demonstrate that GABA$_A$-mediated inhibition most profoundly affects SSA, since co-application of CGP 35348 plus gabazine differs from the application alone of CGP 35348 but not from that of the CGP 35348 plus gabazine plus strychnine (Fig. 6b). This observation is in agreement with the previous studies showing that GABA$_A$ receptors exert a profound change in neuronal firing through a gain control on SSA neurons in the IC (Pérez-González et al. 2012) and auditory thalamus (Duque et al. 2014). Unfortunately, a direct comparison of our results with those obtained by Pérez-González and colleagues is not possible, since we used smaller current injections for gabazine due to the multiple current injects being simultaneously applied to the same neuron.

Finally, both antagonists for GABA$_B$ receptors only increased the late and persistent steady state (A_{ss}, Figs. 7d, 8d, Table 1) but not the initial component of adaptation, revealing that pre- and post-synaptic GABA$_B$ receptors are not involved in the generation of SSA. Furthermore, the lack of effect of GABA$_B$ antagonists on the initial fast (A_r, τ_r) and slow decay (A_s, τ_s) is consistent with the dynamics of activation of metabotropic receptors. Activation of GABA$_B$ receptors is slower than the activation of ionotropic GABA$_A$ receptors, since they are coupled to ion channels via second messengers (Mott 2015). In contrast, gabazine alone (Pérez-González et al. 2012) and combined injections, including the antagonist of GABA$_A$ receptors (Table 1), affected both the decay and sustained components. Gabazine effect is consistent with the blockade of phasic inhibition elicited by fast GABA$_A$-mediated inhibitory postsynaptic potentials that regulate point-to-point communication between neurons.

Overall, our results demonstrate differential roles of pre- and postsynaptic inhibitory receptors in shaping the strength and temporal course of SSA over hundreds of milliseconds and further suggest that other mechanisms participate in the generation of SSA such as adaptation occurring at inputs to SSA neurons (Duque et al. 2016; Nelson and Young 2010).

Compliance with ethical standards

Conflict of interest The authors declare that they have no conflict of interest.

References

Anderson LA, Christianson GB, Linden JF (2009) Stimulus-specific adaptation occurs in the auditory thalamus. J Neurosci 29:7359–7363. https://doi.org/10.1523/JNEUROSCI.0793-09.2009

Antunes FM, Malmierca MS (2011) Effect of auditory cortex deactivation on stimulus-specific adaptation in the medial geniculate body. J Neurosci 31:17306–17316. https://doi.org/10.1523/JNEUROSCI.1915-11.2011

Antunes FM, Nelken I, Covey E, Malmierca MS (2010) Stimulus-specific adaptation in the auditory thalamus of the anesthetized rat. PLoS One 5:e14071. https://doi.org/10.1371/journal.pone.0014071

Ayala YA, Malmierca MS (2013) Stimulus-specific adaptation and deviance detection in the inferior colliculus Front Neural Circuits 6:89. https://doi.org/10.3389/fncir.2012.00089

Ayala YA, Malmierca MS (2014) Cholinergic modulation of stimulus-specific adaptation in the inferior colliculus. In: Paper presented at the 9th FENS forum of neuroscience, Milan

Ayala YA, Malmierca MS (2015) Modulation of auditory deviant saliency in the inferior colliculus. In: Paper presented at the ARO midwinter meeting, Baltimore

Ayala YA, Perez-Gonzalez D, Duque D, Nelken I, Malmierca MS (2013) Frequency discrimination and stimulus deviance in the inferior colliculus and cochlear nucleus. Front Neural Circuits 6:119. https://doi.org/10.3389/fncir.2012.00119

Ayala YA, Udeh A, Dutta K, Bishop D, Malmierca MS, Oliver DL (2015) Differences in the strength of cortical and brainstem inputs to SSA and non-SSA neurons in the inferior colliculus. Sci Rep 5:10383. https://doi.org/10.1038/srep10383

Ayala YA, Pérez-González D, Duque D, Palmer AR, Malmierca MS (2016) Extracellular recording of euronal activity combined with microiontophoretic application of neuroactive substances in awake mice. J Vis Exp. https://doi.org/10.3791/53914

Binns KE, Salt TE (1995) Excitatory amino acid receptors modulate habituation of the response to visual stimulation in the cat superior colliculus. Vis Neurosci 12:563–571

Binns KE, Salt TE (1997) Different roles for GABAA and GABAB receptors in visual processing in the rat superior colliculus. J Physiol 504(Pt 3):629–639

Burger RM, Pollak GD (1998) Analysis of the role of inhibition in shaping responses to sinusoidally amplitude-modulated signals in the inferior colliculus. J Neurophysiol 80:1686–1701

Calford MB (1983) The parcellation of the medial geniculate body of the cat defined by the auditory response properties of single units. J Neurosci 3:2350–2364

Carandini M (2007) Melting the iceberg: contrast invariance in visual cortex. Neuron 54:11–13. https://doi.org/10.1016/j.neuron.2007.03.019

Charara A, Pare JF, Levey AI, Smith Y (2005) Synaptic and extrasynaptic GABA-A and GABA-B receptors in the globus pallidus: an electron microscopic immunogold analysis in monkeys. Neuroscience 131:917–933

Dimitrov AG, Cummins GI, Mayko ZM, Portfors CV (2014) Inhibition does not affect the timing code for vocalizations in the mouse auditory midbrain. Front Physiol 5:140. https://doi.org/10.3389/fphys.2014.00140

Duque D, Malmierca MS (2014) Stimulus-specific adaptation in the inferior colliculus of the mouse: anesthesia and spontaneous activity effects. Brain Struct Funct. https://doi.org/10.1007/s00429-014-0862-1

Duque D, Perez-Gonzalez D, Ayala YA, Palmer AR, Malmierca MS (2012) Topographic distribution, frequency, and intensity dependence of stimulus-specific adaptation in the inferior colliculus of the rat. J Neurosci 32:17762–17774. https://doi.org/10.1523/JNEUROSCI.3190-12.2012

Duque D, Malmierca MS, Caspary DM (2014) Modulation of stimulus-specific adaptation by GABA(A) receptor activation or blockade in the medial geniculate body of the anaesthetized rat. J Physiol 592:729–743. https://doi.org/10.1113/jphysiol.2013.261941

Duque D, Ayala YA, Malmierca MS (2015) Deviance detection in auditory subcortical structures: what can we learn from neurochemistry and neural connectivity? Cell Tissue Res. https://doi.org/10.1007/s00441-015-2134-7

Duque D, Wang X, Nieto-Diego J, Krumbholz K, Malmierca MS (2016) Neurons in the inferior colliculus of the rat show stimulus-specific adaptation for frequency, but not for intensity. Sci Rep 6:24114. https://doi.org/10.1038/srep24114

Eytan D, Brenner N, Marom S (2003) Selective adaptation in networks of cortical neurons. J Neurosci 23:9349–9356

Faingold CL, Boersma Anderson CA, Caspary DM (1991) Involvement of GABA in acoustically-evoked inhibition in inferior colliculus neurons. Hear Res 52:201–216

Faure PA, Fremouw T, Casseday JH, Covey E (2003) Temporal masking reveals properties of sound-evoked inhibition in duration-tuned neurons of the inferior colliculus. J Neurosci 23:3052–3065

Friauf E, Fischer AU, Fuhr MF (2015) Synaptic plasticity in the auditory system: a review. Cell Tissue Res. https://doi.org/10.1007/s00441-015-2176-x

Getting PA (1989) Emerging principles governing the operation of neural networks. Annu Rev Neurosci 12:185–204

Hammond C (2015) The ionotropic GABAA receptor, chap 9. In: Cellular and molecular neurophysiology, 4th edn. Academic Press, Constance Hammond

Hernandez O, Espinosa N, Perez-Gonzalez D, Malmierca MS (2005) The inferior colliculus of the rat: a quantitative analysis of monaural frequency response areas. Neuroscience 132:203–217. https://doi.org/10.1016/j.neuroscience.2005.01.001

Ito T, Bishop DC, Oliver DL (2015) Functional organization of the local circuit in the inferior colliculus. Anat Sci Int. https://doi.org/10.1007/s12565-015-0308-8

Jamal L, Zhang H, Finlayson PG, Porter LA, Zhang H (2011) The level and distribution of the GABA(B)R2 receptor subunit in the rat's central auditory system. Neuroscience 181:243–256. https://doi.org/10.1016/j.neuroscience.2011.02.050

Jamal L, Khan AN, Butt S, Patel CR, Zhang H (2012) The level and distribution of the GABA(B)R1 and GABA(B)R2 receptor subunits in the rat's inferior colliculus. Front Neural Circuits 6:92. https://doi.org/10.3389/fncir.2012.00092

Kelly JB, Caspary DM (2005) Pharmacology of the inferior colliculus. In: Winer JA, Schreiner CE (eds) the inferior colliculus. Springer, New York, pp 248–281

Kraus N, McGee T, Littman T, Nicol T, King C (1994) Nonprimary auditory thalamic representation of acoustic change. J Neurophysiol 72:1270–1277

LeBeau FE, Malmierca MS, Rees A (2001) Iontophoresis in vivo demonstrates a key role for GABA(A) and glycinergic inhibition in shaping frequency response areas in the inferior colliculus of guinea pig. J Neurosci 21:7303–7312

Luo B, Wang HT, Su YY, Wu SH, Chen L (2011) Activation of presynaptic GABAB receptors modulates GABAergic and glutamatergic inputs to the medial geniculate body. Hear Res 280:157–165. https://doi.org/10.1016/j.heares.2011.05.018

Ma CL, Kelly JB, Wu SH (2002) Presynaptic modulation of GABAergic inhibition by GABA(B) receptors in the rat's inferior colliculus. Neuroscience 114:207–215

Magnusson AK, Park TJ, Pecka M, Grothe B, Koch U (2008) Retrograde GABA signaling adjusts sound localization by balancing excitation and inhibition in the brainstem. Neuron 59:125–137. https://doi.org/10.1016/j.neuron.2008.05.011

Malmierca MS, Hernandez O, Rees A (2005) Intercollicular commissural projections modulate neuronal responses in the inferior colliculus. Eur J Neurosci 21:2701–2710. https://doi.org/10.1111/j.1460-9568.2005.04103.x

Malmierca MS, Izquierdo MA, Cristaudo S, Hernandez O, Perez-Gonzalez D, Covey E, Oliver DL (2008) A discontinuous tonotopic organization in the inferior colliculus of the rat. J Neurosci 28:4767–4776. https://doi.org/10.1523/JNEUROSCI.0238-08.2008

Malmierca MS, Cristaudo S, Perez-Gonzalez D, Covey E (2009) Stimulus-specific adaptation in the inferior colliculus of the anesthetized rat. J Neurosci 29:5483–5493. https://doi.org/10.1523/JNEUROSCI.4153-08.2009

Malmierca MS, Blackstad TW, Osen KK (2011) Computer-assisted 3-D reconstructions of Golgi-impregnated neurons in the cortical regions of the inferior colliculus of rat. Hear Res 274(1–2):13–26

Maravall M (2013) Adaptation and sensory coding. In: Quiroga RQ, Panzeri S (eds) Principles of neural coding. CRC Press, Boca Raton, pp 357–377

Merrill EG, Ainsworth A (1972) Glass-coated platinum-plated tungsten microelectrodes. Med Biol Eng 10:662–672

Milbrandt JC, Albin RL, Caspary DM (1994) Age-related decrease in GABAB receptor binding in the Fischer 344 rat inferior colliculus. Neurobiol Aging 15:699–703

Mott D (2015) The metabotropic GABAB receptors, chapter 11. In: Cellular and molecular neurophysiology, 4th edn. Academic Press, Constance Hammond

Näätänen R (1992) Attention and brain function. Lawrence Erlbaum, Hillsdale

Nelken I (2014) Stimulus-specific adaptation and deviance detection in the auditory system: experiments and models. Biol Cybern 108:655–663. https://doi.org/10.1007/s00422-014-0585-7

Nelson PC, Young ED (2010) Neural correlates of context-dependent perceptual enhancement in the inferior colliculus. J Neurosci 30:6577–6587. https://doi.org/10.1523/JNEUROSCI.0277-10.2010

Nieto-Diego J, Malmierca MS (2016) Topographic distribution of stimulus-specific adaptation across auditory cortical fields in the anesthetized rat. PLoS Biol 14:1002397. https://doi.org/10.1371/journal.pbio.1002397

Olpe HR et al (1990) CGP 35348: a centrally active blocker of GABAB receptors. Eur J Pharmacol 187:27–38

Ong J, Bexis S, Marino V, Parker DA, Kerr DI, Froestl W (2001) CGP 36216 is a selective antagonist at GABA(B) presynaptic receptors in rat brain. Eur J Pharmacol 415:191–195

Oyster CW, Takahashi ES (1975) Responses of rabbit superior colliculus neurons to repeated visual stimuli. J Neurophysiol 38:301–312

Pérez-González D, Malmierca MS (2012) Variability of the time course of stimulus-specific adaptation in the inferior colliculus. Front Neural Circuits 6:107. https://doi.org/10.3389/fncir.2012.00107

Pérez-González D, Malmierca MS, Covey E (2005) Novelty detector neurons in the mammalian auditory midbrain. Eur J Neurosci 22:2879–2885. https://doi.org/10.1111/j.1460-9568.2005.04472.x

Pérez-González D, Malmierca MS, Moore JM, Hernandez O, Covey E (2006) Duration selective neurons in the inferior colliculus of the rat: topographic distribution and relation of duration sensitivity to other response properties. J Neurophysiol 95:823–836. https://doi.org/10.1152/jn.00741.2005

Pérez-González D, Hernandez O, Covey E, Malmierca MS (2012) GABA(A)-mediated inhibition modulates stimulus-specific adaptation in the inferior colliculus. PLoS One 7:e34297. https://doi.org/10.1371/journal.pone.0034297

Pham TM, Nurse S, Lacaille J-C (1998) Distinct GABAB actions via synaptic and extrasynaptic receptors in rat hippocampus in vitro. J Neurophysiol 80:297–308

Rees A (1990) A close-field sound system for auditory neurophysiology. J Physiol 430:6

Scanziani M (2000) GABA spillover activates postsynaptic GABA(B) receptors to control rhythmic hippocampal activity. Neuron 25:673–681

Sivaramakrishnan S, Sterbing-D'Angelo SJ, Filipovic B, D'Angelo WR, Oliver DL, Kuwada S (2004) GABA(A) synapses shape neuronal responses to sound intensity in the inferior colliculus. J Neurosci 24:5031–5043. https://doi.org/10.1523/JNEUROSCI.0357-04.2004

Staubli U, Scafidi J, Chun D (1999) GABAB receptor antagonism: facilitatory effects on memory parallel those on LTP induced by TBS but not HFS. J Neurosci 19:4609–4615

Sun H, Wu SH (2008) Physiological characteristics of postinhibitory rebound depolarization in neurons of the rat's dorsal cortex of the inferior colliculus studied in vitro. Brain Res 1226:70–81. https://doi.org/10.1016/j.brainres.2008.06.010

Sun H, Wu SH (2009) The physiological role of pre- and postsynaptic GABA(B) receptors in membrane excitability and synaptic transmission of neurons in the rat's dorsal cortex of the inferior colliculus. Neuroscience 160:198–211. https://doi.org/10.1016/j.neuroscience.2009.02.011

Sun H, Ma CL, Kelly JB, Wu SH (2006) GABAB receptor-mediated presynaptic inhibition of glutamatergic transmission in the inferior colliculus. Neurosci Lett 399:151–156. https://doi.org/10.1016/j.neulet.2006.01.049

Ulanovsky N, Las L, Nelken I (2003) Processing of low-probability sounds by cortical neurons. Nat Neurosci 6:391–398. https://doi.org/10.1038/nn1032

Ulanovsky N, Las L, Farkas D, Nelken I (2004) Multiple time scales of adaptation in auditory cortex neurons. J Neurosci 24:10440–10453. https://doi.org/10.1523/JNEUROSCI.1905-04.2004

Valdés-Baizabal C, Parras GG, Ayala YA, Malmierca MS (2017) Endocannabinoid modulation of stimulus-specific adaptation in inferior colliculus neurons of the rat. Scientific Rep 7(1). https://doi.org/10.1038/s41598-017-07460-w

Vaughn MD, Pozza MF, Lingenhöhl K (1996) Excitatory acoustic responses in the inferior colliculus of the rat are increased by GABAB receptor blockade. Neuropharmacology 35(12):1761–1767

von der Behrens W, Bauerle P, Kossl M, Gaese BH (2009) Correlating stimulus-specific adaptation of cortical neurons and local field potentials in the awake rat. J Neurosci 29:13837–13849. https://doi.org/10.1523/JNEUROSCI.3475-09.2009

Wang H, Han Y-F, Chan Y-S, He J (2014) Stimulus-specific adaptation at the synapse level in vitro. PLoS One 9(12):114537. https://doi.org/10.1371/journal.pone.0114537

Williams AJ, Fuzessery ZM (2011) Differential roles of GABAergic and glycinergic input on FM selectivity in the inferior colliculus of the pallid bat. J Neurophysiol 106:2523–2535. https://doi.org/10.1152/jn.00569.2011

Winkler I, Denham SL, Nelken I (2009) Modeling the auditory scene: predictive regularity representations and perceptual objects. Trends Cognit Sci 13:532–540. https://doi.org/10.1016/j.tics.2009.09.003

Zhang Y, Wu SH (2000) Long-term potentiation in the inferior colliculus studied in rat brain slice. Hear Res 147:92–103